



# Electrical and sensing properties of a flexible humidity sensor made of polyamidoamine dendrimer-Au nanoparticles

Pi-Guey Su\*, Chuen-Chi Shiu

Department of Chemistry, Chinese Culture University, Taipei 111, Taiwan

## ARTICLE INFO

### Article history:

Received 19 November 2011  
 Received in revised form 1 February 2012  
 Accepted 13 February 2012  
 Available online 21 February 2012

### Keywords:

Flexible  
 Humidity sensor  
 G1-NH<sub>2</sub>-AuNPs  
 Impedance analysis  
 Sensing properties

## ABSTRACT

Generation 1 amine terminated polyamidoamine (PAMAM) dendrimer (G1-NH<sub>2</sub>)-Au nanoparticles (G1-NH<sub>2</sub>-AuNPs) was coated on a polyester (PET) substrate to form a novel flexible impedance-type humidity sensor. The formation of AuNPs was characterized by UV-vis spectroscopy. The microstructure of the G1-NH<sub>2</sub>-AuNPs film was analyzed by atomic force microscope (AFM). The effect of the AuNPs on the electrical and humidity sensing properties of the G1-NH<sub>2</sub>-AuNPs films on a PET substrate was investigated. The sensor had good flexibility. This flexible humidity sensor also exhibited good sensitivity and acceptable linearity ( $Y = -0.045X + 7.866$ ;  $R^2 = 0.9693$ ) between logarithmic impedance ( $\log Z$ ) and RH in the range 30–90%RH, negligible hysteresis (within 2%RH), good response time (40 s) and recovery time (50 s), and long-term stability (39 days at least), measured at 1 V, 1 kHz and 25 °C. The flexible humidity sensor's linearity depended on the applied frequency. The temperature influence between 15 and 35 °C; found to be  $-0.55\%RH/^\circ C$  for 30–90%RH. The different complex impedance plots obtained at low and high relative humidity indicated that the ions dominate the conductance of the G1-NH<sub>2</sub>-AuNPs film.

© 2012 Elsevier B.V. All rights reserved.

## 1. Introduction

Flexible sensors has attracted much interest recently because of they have light weight, robustness, low cost and flexible, making them suitable for application in various new areas, such as handheld portable consumer electronics, smart textiles and radio frequency identification (RFID) tags [1–4]. The main challenge for development of flexible sensors is not only their manufacture, but also the stability of their mechanical, electrical and sensing properties under repeated bending.

Humidity sensors are widely used in measurement and control of humidity in human comfort and a myriad of industrial processes. Many materials have been studied for their use in fabricating humidity sensors, including polymers, ceramics and composites. Polymers are widely employed as practical humidity sensors [5–9], since they present many advantages such as low cost, flexibility and easy processability. Flexible humidity sensors, fabricated from polymeric materials, have recently been divided into two categories of capacitive-type and impedance-type [10–15]. Oprea et al. developed capacitive-type humidity sensors that were integrated into a flexible RFID tag, based on polycellulose acetate (PCA), polycelluloseacetate-butyrate (PCAB), polymethyl-methacrylate (PMMA) and polyvinylpyrrolidone

(PVP) sensing films [10]. Zampetti et al. fabricated a flexible capacitive-type humidity sensor that was made by coating a bis(benzo-cyclobutene) (BCB) film on a polyimide substrate [11]. In our earlier studies [12–15], flexible impedance-type humidity sensors that were made by coating the copolymer of methyl methacrylate (MMA) and [3-(methacrylamino)propyl] trimethyl ammonium chloride (MAPTAC) (poly-MMA/MAPTAC) [12,13], TiO<sub>2</sub> nanoparticles-polypyrrole-poly-[3-(methacrylamino)propyl] trimethyl ammonium chloride composite material [14] and poly(2-acrylamido-2-methylpropane sulfonate) (PAMPS) and its salt complex [15] sensing films on a flexible substrate (polyester film; PET).

Au nanoparticles (AuNPs) have attracted much interest because of their attractive electronic, unique optical, thermal and physical properties as well as their catalytic activity and potential applications in chemical sensors and biosensors [16]. Polyamidoamine (PAMAM) dendrimers are highly branched and well-defined three-dimensional macromolecules [17]. They have attracted much interest recently because of their high geometric symmetry, easily controlled nanosize, controllable surface functionality, film-forming ability and chemical stability, which have resulted in the extension of their use to biosensors and chemical sensors [18–22]. Grabchev et al. synthesized 1,8-naphthalimide-labeled PAMAM for the detection of transition metal ions [18]. Kwak et al. prepared a hydrogen peroxide sensor by depositing Prussian blue on nano-Au/PAMAM dendrimer-modified gold electrode [19]. Yang et al. fabricated an impedimetric thrombin aptasensor

\* Corresponding author. Tel.: +886 2 28610511x25332; fax: +886 2 28614212.  
 E-mail addresses: [spg@faculty.pccu.edu.tw](mailto:spg@faculty.pccu.edu.tw), [spg@ulive.pccu.edu.tw](mailto:spg@ulive.pccu.edu.tw) (P.-G. Su).

that was based on a PAMAM dendrimer-modified gold electrode [20]. Shi et al. fabricated a carbofuran sensor made of acetylcholinesterase/PAMAM-Au on a CNT-modified electrode by layer-by-layer self-assembly [21]. Zhu et al. fabricated a bisphenol (BPA) sensor that was made of a PAMAM dendrimer and a CoTe quantum dots-modified glassy carbon electrode [22]. However, no attempt has been made to construct flexible impedance-type polymeric humidity sensors based on PAMAM dendrimers. In this study, generation 1 amine terminated PAMAM dendrimer (G1-NH<sub>2</sub>) and G1-NH<sub>2</sub>-Au nanoparticles (G1-NH<sub>2</sub>-AuNPs) were drop-coated on a polyester (PET) substrate to form flexible impedance-type humidity sensors. The G1-NH<sub>2</sub>-AuNPs were characterized using an atomic force microscope (AFM) and a UV-vis spectrophotometer. The effect of the AuNPs in the G1-NH<sub>2</sub>-AuNPs film on the response of the film to a change in humidity was investigated. The flexibility and humidity-sensing properties, including sensitivity, hysteresis, effects of applied frequency and ambient temperature, response time, recovery time and stability were also investigated. The complex impedance spectra were used to elucidate the sensing mechanism of the G1-NH<sub>2</sub>-AuNPs film.

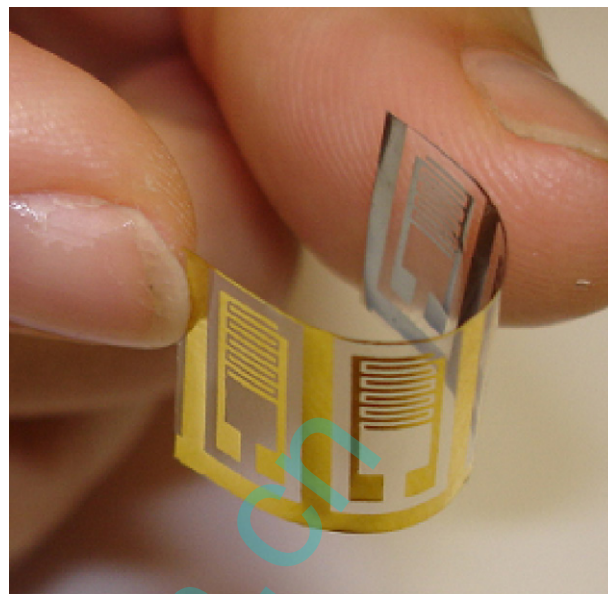


Fig. 1. Photo of humidity sensors on a PET substrate.

## 2. Experimental

### 2.1. Preparation of humidity sensor

Fig. 1 displays a picture of the structure of humidity sensors fabricated on a PET substrate. The interdigitated gold electrodes were made by sputtering initially Cr (thickness 50 nm) and then Au (thickness 250 nm) in a temperature range of 120–160 °C. The electrode gap was 0.2 mm.

G1-NH<sub>2</sub> dendrimer (5 wt% in methanol solution, Aldrich) was used without further purification. The preparation of G1-NH<sub>2</sub>-AuNPs solution was similar to the method that was reported by Shi et al. [21]. G1-NH<sub>2</sub>-AuNPs solution was prepared by adding 5 mL of 20 or 50 mg/mL of HAuCl<sub>4</sub> solution to 0.1 mL of G1-NH<sub>2</sub>, stirring for 20 min, and then incrementally adding an excess of formic acid (reducing agent, 4.0 mM) into the solution to ensure that most of the HAuCl<sub>4</sub> was reduced to AuNPs. When the AuNPs were formed, the color changed from yellow to wine-red. The G1-NH<sub>2</sub>-AuNPs solution was drop-coated on a PET substrate containing a pair of interdigitated gold electrodes, followed by heating at 60 °C for 5 min in air. Thus a flexible impedance-type humidity sensor was obtained.

### 2.2. Instruments and analysis

The formation of AuNPs was characterized by UV-vis spectroscopy (Agilent 8453). The surface microstructure of the G1-NH<sub>2</sub>-AuNPs thin films that was coated on a substrate was investigated using an atomic force microscope (AFM, Ben-Yuan, CSPM 4000) in tapping mode. Impedance of a sensor as a function of RH was measured with an LCR meter (Philips PM6306) in a test chamber under the conditions of a measurement frequency of 1 kHz, an applied voltage of 1 V, an ambient temperature of 25 °C. A frequency range of 50 Hz to 100 kHz, an RH range from 30 to 90% at 25 °C and an applied voltage of 1 V were used in the complex impedance analysis. As shown in Fig. 2, a divided humidity generator was used for producing the testing gases using of mass flow controllers (Hastings), as described elsewhere [23]. The required humidity was produced by adjusting the proportion of dry and humid air generated by the divided flow humidity generator under a total flow rate is 10 L/min. The setting humidity and temperature points were calibrated by using a standard hygrometer (Rotronic Inc) with an accuracy of ±0.1%RH which was pre-calibrated in

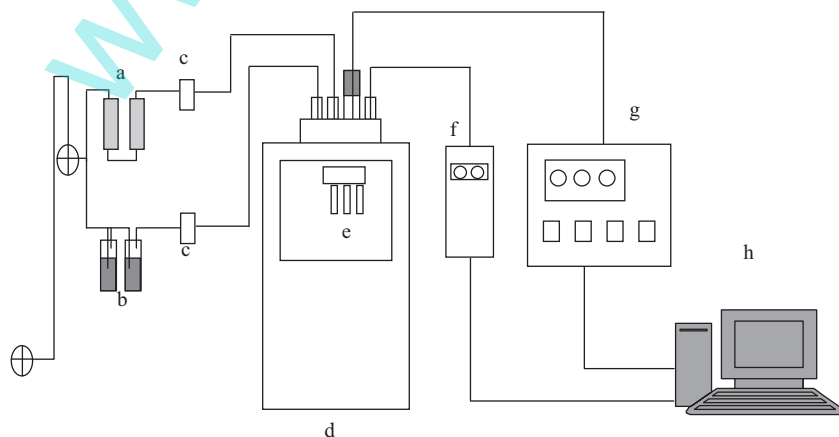
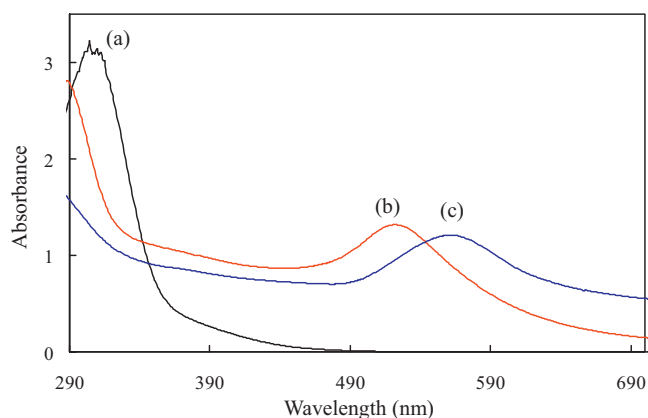


Fig. 2. Schematic plot of the impedance measurement of sensors and the humidity atmosphere controller. (a) Molecular sieve and desiccating agent; (b) water; (c) mass flow controller; (d) controlled temperature detection chamber; (e) humidity sensor; (f) hygrometer; (g) LCR meter; and (h) PC.



**Fig. 3.** UV-vis absorption spectra of (a) G1-NH<sub>2</sub>-HAuCl<sub>4</sub> solution; (b) G1-NH<sub>2</sub>-AuNPs with 20 mg/mL added HAuCl<sub>4</sub>; and (c) G1-NH<sub>2</sub>-AuNPs with 50 mg/mL added HAuCl<sub>4</sub>.

the National Measurement Laboratory (NML) humidity laboratory. Flexibility experiments were performed in which the sensor was bent to various degrees as their responses were monitored as a function of the period of exposure to humidity. The bending angle was measured using a goniometer.

### 3. Results and discussion

#### 3.1. Characteristics of G1-NH<sub>2</sub>-AuNPs

Fig. 3 shows the UV-vis absorption of G1-NH<sub>2</sub>-encapsulated AuNPs. The G1-NH<sub>2</sub>-HAuCl<sub>4</sub> solution had a ligand-metal charge-transfer band at 300 nm (curve a). Curves b and c are the absorption spectra of the after reduction of the G1-NH<sub>2</sub>-HAuCl<sub>4</sub> solution using 20 and 50 mg/mL added HAuCl<sub>4</sub>, respectively. Both curves b and c are higher at higher wavelengths, resulting from the inter-band transition of the encapsulated AuNPs. The absorption band of curve c (560 nm) was longer and broader than that of curve b (524 nm). Ghost and Pal pointed out that the absorption band of AuNPs was red-shifted as the size of the AuNPs increased or the AuNPs aggregated [24]. Therefore, the above result is attributable to the enlargement or aggregation of AuNPs upon the addition of 50 mg/mL of HAuCl<sub>4</sub>. When more than 50 mg/mL HAuCl<sub>4</sub> was added, encapsulated AuNPs clearly precipitated out of G1-NH<sub>2</sub>-AuNPs solution.

#### 3.2. Surface microstructure of G1-NH<sub>2</sub>-AuNPs film

The surface morphology of the G1-NH<sub>2</sub>-AuNPs films with various amount of added HAuCl<sub>4</sub> was analyzed using tapping mode AFM. Fig. 4(a) and (b) presents the surface images of the G1-NH<sub>2</sub>-AuNPs films with addition of 20 and 50 mg/mL HAuCl<sub>4</sub>, respectively. The formation of AuNPs that were encapsulated in G1-NH<sub>2</sub> and some free AuNPs were found on the film (Fig. 4(a) and (b)). The data of the root mean square (RMS) roughness of the G1-NH<sub>2</sub>-AuNPs film (11.5 nm) with addition of 50 mg/mL HAuCl<sub>4</sub> was higher than that of the film (7.3 nm) with addition of 20 mg/mL HAuCl<sub>4</sub>. Additionally, obvious aggregation of AuNPs occurred on the G1-NH<sub>2</sub>-AuNPs film with addition of 50 mg/mL of HAuCl<sub>4</sub> (Fig. 4(b)).

#### 3.3. Flexibility and humidity sensing properties of G1-NH<sub>2</sub>-AuNPs films

The effect of adding AuNPs on the electrical response of G1-NH<sub>2</sub>-AuNPs films was measured at various relative humidities. The measurements were made at 25 °C using an AC voltage of

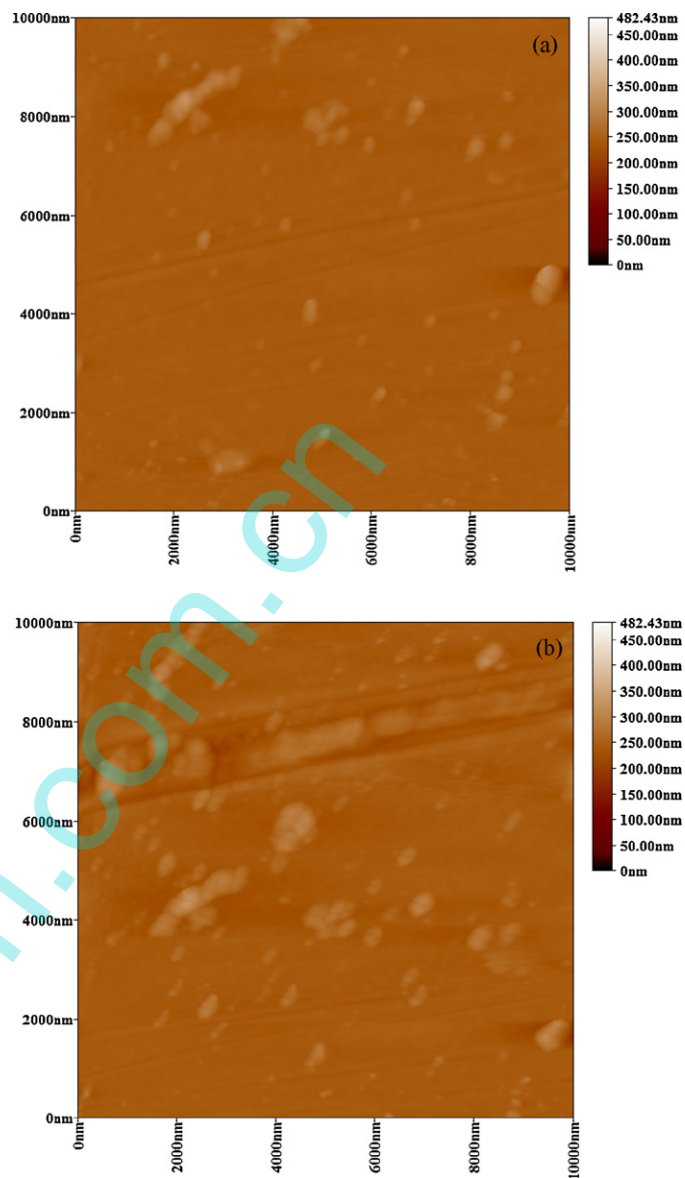


**Fig. 4.** AFM images of G1-NH<sub>2</sub>-AuNPs film (a) with 20 mg/mL added HAuCl<sub>4</sub>; and (b) with 50 mg/mL added HAuCl<sub>4</sub>.

1 V, at 1 kHz. These results are plotted in Fig. 5. G1-NH<sub>2</sub> film exhibited an impedance change in the range 70–90%RH, and almost no impedance change occurred in the range of 30–70%RH. PAMAM dendrimers are highly branched well-defined three-dimensional macromolecules with hydrophilic terminal functional groups (–NH<sub>2</sub>) and hydrophobic interior layers at the core. Therefore, ion conduction in the G1-NH<sub>2</sub> film occurs mainly at the outermost layer, and the number of mobile ions in the internal layers was very small, so the impedance of the G1-NH<sub>2</sub> film in the range 30–70%RH was high. When the G1-NH<sub>2</sub> was doped with AuNPs, the impedance of the G1-NH<sub>2</sub>-AuNPs film was markedly reduced over a wide range of RH. Additionally, the impedance of the G1-NH<sub>2</sub>-AuNPs film with 50 mg/mL added HAuCl<sub>4</sub> was decreased over a wider range of RH (30–90%RH) than was that of the film with 20 mg/mL added HAuCl<sub>4</sub>, suggesting that the former had the highest sensitivity and the best linear response curve. These results are attributed to the fact that AuNPs in the G1-NH<sub>2</sub>-AuNPs film had an important role, as a conducting wire, in facilitating the transfer of charge carriers [19,21]. Therefore, the G1-NH<sub>2</sub>-AuNPs film

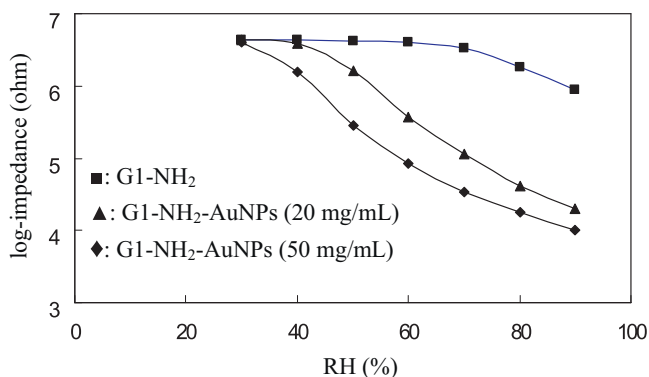


Fig. 5. Impedance versus relative humidity for G1-NH<sub>2</sub> and G1-NH<sub>2</sub>-AuNPs films, measured at 1 kHz, 1 V and 25 °C.

with 50 mg/mL added HAuCl<sub>4</sub> was further tested to evaluate its flexibility and humidity-sensing characteristics.

The flexibility characteristics of the G1-NH<sub>2</sub>-AuNPs film as humidity sensor are shown in Fig. 6. The sensor response (*S*) was calculated, according to  $S = (\log Z_{30\%RH} - \log Z_{60\%RH}) / \log Z_{30\%RH} \times 100\%$ , ( $\Delta Z / \log Z_{30\%RH} \times 100\%$ ), where  $Z_{30\%RH}$  and  $Z_{60\%RH}$  are the impedance of the transparent humidity sensor at 30 and 60%RH, respectively. At each bending angle, the sensor was exposed to 60%RH. The sensor response deviation (*D*) was calculated, according to  $D = (S_f - S_b) / S_f \times 100\%$ , where  $S_f$  and  $S_b$  are the response of the flexible humidity sensor at flat and bending, respectively. When the sensor was bent downward at an angle of up to 60°, the response deviation was within <2%. These results indicate that even under an applied stress, the sensor was sufficiently flexible and exhibited good electrical performance when it was bent.

Fig. 7 shows the log-impedance of the flexible humidity sensor as a function of RH. The measurements were made at 25 °C using an AC voltage of 1 V, at 1 kHz. The open symbols in figure represent measurements during desiccation, while solid symbols are for humidification. The impedance changed from 10<sup>6</sup> to 10<sup>4</sup> Ω and the curves reveal satisfactorily linear relationship ( $Y = -0.045X + 7.866$ ;  $R^2 = 0.9693$ ) between log-impedance and RH in the range 30–90%RH. However, almost no impedance changed in the range of 10–30%RH (shown in the inset). The hysteresis (between humidification and desiccation, measured over an RH range of 30–90%RH) was less than 2%RH.

Fig. 8 shows the log-impedance of the flexible sensor as a function of measurement frequency at various RH values. The measurements were made at 25 °C using an AC voltage of 1 V. The frequency clearly affected the humidity-dependence of the impedance of the flexible sensor. The impedance decreased as the

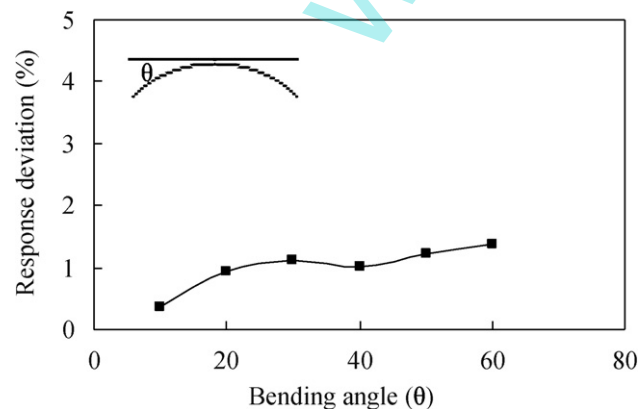


Fig. 6. Flexible characteristics of G1-NH<sub>2</sub>-AuNPs film with 50 mg/mL added HAuCl<sub>4</sub>.

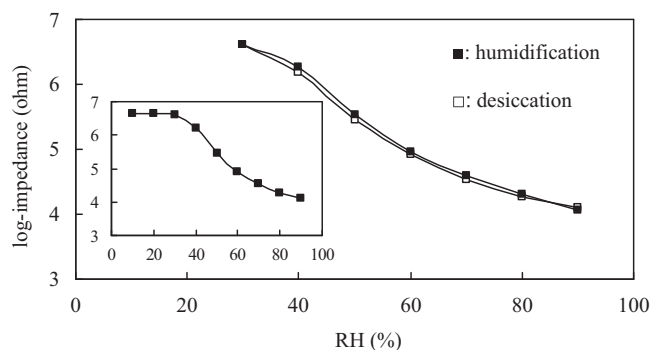


Fig. 7. Impedance versus relative humidity for G1-NH<sub>2</sub>-AuNPs film with 50 mg/mL added HAuCl<sub>4</sub>, measured at 1 kHz, 1 V and 25 °C.

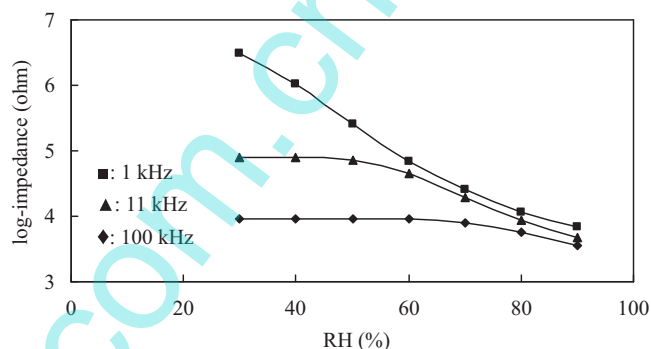


Fig. 8. Impedance versus relative humidity for G1-NH<sub>2</sub>-AuNPs film with 50 mg/mL added HAuCl<sub>4</sub> at various frequencies.

frequency increased, and the curve of impedance was most linear at 1 kHz. The log-impedance was almost flat above 11 kHz. At a very high frequency, the direction of the electrical field changed rapidly, and the change in the orientation of the adsorbed water could not keep up with this change. Therefore, the dielectric character was weak and independent of RH [25].

The log-impedance of the flexible humidity sensor was dependent on the ambient temperatures, as shown in Fig. 9. As the temperature increased, the RH characteristic curve shifted toward lower impedance. The mean temperature coefficient at 15–35 °C was  $-0.55\%RH/^{\circ}C$  over the humidity range 30–90%RH.

The response–recovery property of the flexible humidity sensor was measured at 25 °C and 1 kHz and shown in Fig. 10. The response time ( $T_{res.95\%}$ ) is defined as the time required for the impedance of the sensor to change by 95% of the maximum change following humidification from 20 to 85%RH. The recovery time ( $T_{rec.95\%}$ ) is defined as the time required for the sensor to recover 95% of

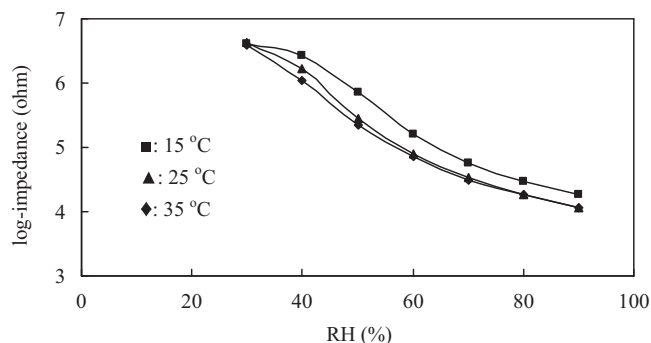
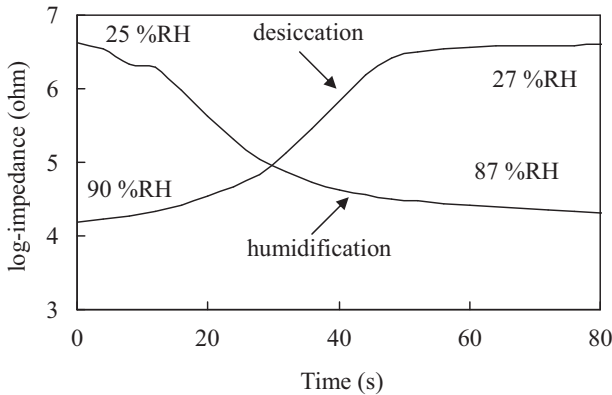


Fig. 9. Impedance versus relative humidity for G1-NH<sub>2</sub>-AuNPs film with 50 mg/mL added HAuCl<sub>4</sub> at various temperatures, measured at 1 V and 1 kHz.

**Table 1**  
Flexible humidity sensor performance of this work compared with the literatures.

Sensing material	Working range (%RH)	Sensitivity (log Z/%RH) <sup>a</sup>	Hysteresis (%RH)	Response time (s)	References
PAMAM-AuNPs	30–90	0.045	<2	40	This work
PMMA/PMAPTAC	30–90	0.033	<6	45	[12]
TiO <sub>2</sub> NPs/PPy/PMAPTAC	30–90	0.065	<2	30	[14]
PAMPS doped salts	20–90	0.026	<8	60	[15]

<sup>a</sup> The sensitivity shown as the slope of the sensing curve in the working range.



**Fig. 10.** Response–recovery properties of G1-NH<sub>2</sub>-AuNPs film with 50 mg/mL added HAuCl<sub>4</sub>, measured at 1 V, 1 kHz and 25 °C.

the maximum change in impedance after desiccation from 90 to 20%RH. The response time ( $T_{res,95\%}$ ) and recovery ( $T_{rec,95\%}$ ) time of the sensor were 40 and 50 s, respectively. The long-term stability is shown in Fig. 11. The flexible sensor impedance did not significantly vary for at least 39 days at the tested RH values of 30, 60, and 90%RH. The humidity-sensing properties of the present flexible humidity sensor were compared with our earlier studies [12,14,15] in Table 1.

### 3.4. Sensing mechanism of G1-NH<sub>2</sub>-AuNPs film

Impedance spectroscopy is a powerful method for elucidating the conduction mechanisms of humidity sensors. Therefore, the obtained impedance plots were utilized to elucidate the transport of ions as a mechanism of conduction in the G1-NH<sub>2</sub>-AuNPs film. The complex impedance spectra of the G1-NH<sub>2</sub>-AuNPs film at various humidities are shown in Fig. 12. The impedance measurements were made in a frequency range from 50 Hz to 100 kHz and humidities from 30 to 90%RH, an AC voltage of 1 V and 25 °C. At low RH (30%RH), a semicircular plot of film impedance was obtained. The semicircle plot of the impedance have been explained by many authors [26–28], resulting mainly from the impedance of the G1-NH<sub>2</sub>-AuNPs film, and the film could be modeled as an

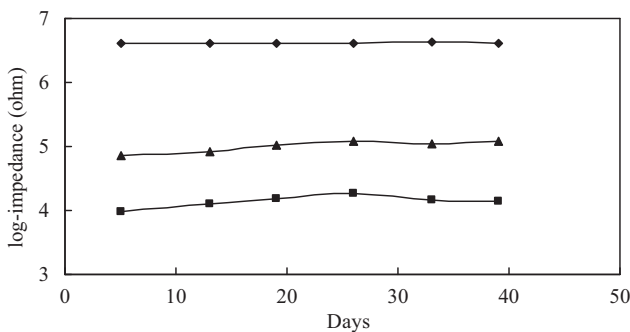


**Fig. 11.** Long-term stability of G1-NH<sub>2</sub>-AuNPs film with 50 mg/mL added HAuCl<sub>4</sub>, measured at 1 V, 1 kHz and 25 °C. 30%RH (◆); 60%RH (▲) and 90%RH (■).

equivalent parallel circuit that incorporates a resistor and a capacitor. As RH increased to 60%RH, a semicircle (at high frequencies) connected with a straight line (at low frequency) was observed. The G1-NH<sub>2</sub>-AuNPs film absorbed more water molecules so that the small film impedance was observed and the semicircle was small. Moreover, RH increased to very high (90%RH), the semicircle was invisible and only a straight line was observed. The straight line at low frequencies was caused by the diffusion of ions (H<sub>3</sub>O<sup>+</sup>) across the interface between the electrode and the G1-NH<sub>2</sub>-AuNPs film. Therefore, these results suggest that the sensing mechanism of the G1-NH<sub>2</sub>-AuNPs film was ionic conductivity.

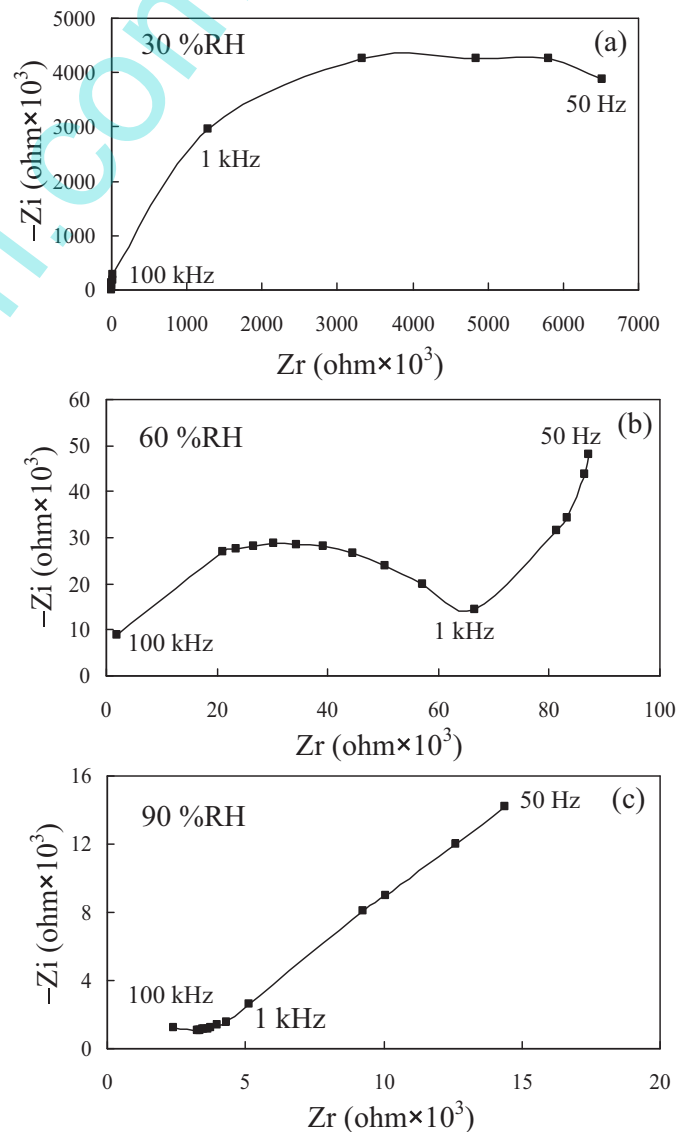


**Fig. 12.** Complex impedance plots of G1-NH<sub>2</sub>-AuNPs film with 50 mg/mL added HAuCl<sub>4</sub> at (a) 30%RH; (b) 60%RH; and (c) 90%RH.

#### 4. Conclusions

The flexible impedance-type humidity sensor based on G1-NH<sub>2</sub> film had a small working range of humidity (70–90%RH) because of the low ion mobility through the interlayer of the G1-NH<sub>2</sub> at low humidity (<70%RH). Doping the G1-NH<sub>2</sub> film with AuNPs, greatly improved the humidity sensing properties of the sensor because that the introduction of AuNPs effectively increased the conductance of the G1-NH<sub>2</sub>-AuNPs film at low RH.

The flexible impedance-type humidity sensor that was based on G1-NH<sub>2</sub>-AuNPs film had a wide working range of humidity (30–90%RH), a high sensitivity, an acceptable linearity, a small hysteresis, high flexibility, a fast response time, a weak dependence on temperature and good long-term stability. The frequency-dependence of the impedance was stronger at lower RH. The plots of the complex impedance of the G1-NH<sub>2</sub>-AuNPs film in different RH showed that the curves changed from semicircular to linear as RH increased. These results reflect the contribution of ions to the conductivity of G1-NH<sub>2</sub>-AuNPs film.

#### Acknowledgement

The authors thank the National Science Council (Grant No. NSC 100-2113-M-034-001-MY3) of Taiwan for support.

#### References

- [1] E. Abad, S. Zampolli, S. Macro, A. Scorzoni, B. Mazzolai, A. Juarros, D. Gómez, I. Elmi, G.C. Cardinali, J.M. Gómez, F. Palacio, M. Cicioni, A. Mondini, T. Becker, I. Sayhan, Flexible tag microlab development: gas sensors integration in RFID flexible tags for food logistic, *Sens. Actuators B* 127 (2007) 2–7.
- [2] A. Vergara, E. Llobet, J.L. Ramírez, P. Ivanov, L. Fonseca, S. Zampolli, A. Scorzoni, T. Becker, S. Marco, J. Wöllenstein, An RFID reader with onboard sensing capability for monitoring fruit quality, *Sens. Actuators B* 127 (2007) 143–149.
- [3] M.C. Mcalpine, H. Ahmad, D. Wang, J.R. Heath, Highly ordered nanowire arrays on plastic substrates for ultrasensitive flexible chemical sensors, *Nat. Mater.* 16 (2007) 379–384.
- [4] Y. Sun, H.H. Wang, High-performance, flexible hydrogen sensors that use carbon nanotubes decorated with palladium nanoparticles, *Adv. Mater.* 19 (2007) 2818–2823.
- [5] Y. Sakai, Y. Sadaoka, M. Matsuguchi, Humidity sensors based on polymer thin films, *Sens. Actuators B* 35–36 (1996) 85–90.
- [6] J. Wang, B. Xu, J. Zhang, G. Liu, T. Zhang, F. Qiu, M. Zhao, Humidity sensors of composite material of nanocrystal BaTiO<sub>3</sub> and polymer (R)<sub>n</sub>M<sup>+</sup>X<sup>-</sup>, *J. Mater. Sci. Lett.* 18 (1999) 1603–1605.
- [7] Y. Sakai, M. Matsuguchi, T. Hurokawa, Humidity sensor using crosslinked poly(chloromethyl styrene), *Sens. Actuators B* 66 (2000) 135–138.
- [8] M.S. Gong, H.W. Rhee, M.H. Lee, Humidity sensor using epoxy resin containing quaternary ammonium salts, *Sens. Actuators B* 73 (2001) 124–129.
- [9] Y. Li, M.J. Yang, Y. She, Humidity sensors using in situ synthesized sodium polystyrenesulfonate/ZnO nanocomposites, *Talanta* 62 (2004) 707–712.
- [10] A. Oprea, N. Bârsan, U. Weimar, M.-L. Bauersfeld, D. Ebling, J. Wöllenstein, Capacitive humidity sensors on flexible RFID labels, *Sens. Actuators B* 132 (2008) 404–410.
- [11] E. Zampetti, S. Pantalei, A. Pecora, A. Valletta, L. Maiolo, A. Minotti, A. Macagnano, G. Fortunato, A. Bearzotti, Design and optimization of an ultra thin flexible capacitive humidity sensor, *Sens. Actuators B* 143 (2009) 302–307.
- [12] P.G. Su, C.S. Wang, Novel flexible resistive-type humidity sensor, *Sens. Actuators B* 123 (2007) 1071–1076.
- [13] P.G. Su, J.Y. Tseng, Y.C. Huang, H.H. Pan, P.C. Li, Novel fully transparent and flexible humidity sensor, *Sens. Actuators B* 137 (2009) 496–500.
- [14] P.G. Su, C.P. Wang, Flexible humidity sensor based on TiO<sub>2</sub> nanoparticles-polyppyrrrole-poly-[3-(methacrylamino)propyl] trimethyl ammonium chloride composite materials, *Sens. Actuators B* 129 (2008) 538–543.
- [15] P.G. Su, W.C. Li, J.Y. Tseng, C.J. Ho, Fully transparent and flexible humidity sensors fabricated by layer-by-layer self-assembly of thin film of poly(2-acrylamido-2-methylpropane sulfonate) and its salt complex, *Sens. Actuators B* 153 (2011) 29–36.
- [16] S. Guo, E. Wang, Synthesis and electrochemical applications of gold nanoparticles, *Anal. Chim. Acta* 598 (2007) 181–192.
- [17] S.M. Grayson, J.M.J. Frechet, Convergent dendrons and dendrimers: from synthesis to applications, *Chem. Rev.* 101 (2001) 3819–3868.
- [18] I. Grabchev, X. Qian, V. Bojinov, Y. Xiao, W. Zhang, Synthesis and photophysical properties of 1,8-naphthalimide-labelled PAMAM as PET sensors of protons and of transition metal ions, *Polymer* 43 (2002) 5731–5736.
- [19] N.B. Li, J.H. Park, K. Park, S.J. Kwon, H. Shin, J. Kwak, Characterization and electrocatalytic properties of Prussian blue electrochemically deposited on nano-Au/PAMAM dendrimer-modified gold electrode, *Biosens. Bioelectron.* 23 (2008) 1519–1526.
- [20] Z. Zhang, W. Yang, J. Wang, C. Yang, F. Yang, X. Yang, A sensitive impedimetric thrombin aptasensor based on polyamidoamine dendrimer, *Talanta* 78 (2009) 1240–1245.
- [21] Y. Qu, Q. Sun, F. Xiao, G. Shi, L. Jin, Layer-by-layer self-assembled acetylcholinesterase/PAMAM-Au on CNTs modified electrode for sensing pesticides, *Bioelectrochemistry* 77 (2010) 139–144.
- [22] H. Yin, Y. Zhou, S. Ai, Q. Chen, X. Zhu, X. Liu, L. Zhu, Sensitivity and selectivity determination of BPA in real water samples using PAMAM dendrimer and CoTe quantum dots modified glassy carbon electrode, *J. Hazard. Mater.* 174 (2010) 236–243.
- [23] P.G. Su, I.C. Chen, R.J. Wu, Use of poly(2-acrylamido-2-methylpropane sulfonate) modified with tetraethyl orthosilicate as sensing material for measurement of humidity, *Anal. Chim. Acta* 449 (2001) 103–109.
- [24] S.K. Ghost, T. Pal, Interparticle coupling effect on the surface plasmon resonance of gold nanoparticles: from theory to applications, *Chem. Rev.* 107 (2007) 4797–4862.
- [25] J. Wang, K. Shi, L. Chen, X. Zhang, Study of polymer humidity sensor array on silicon wafer, *J. Mater. Sci.* 39 (2004) 3155–3157.
- [26] C.D. Feng, S.L. Sun, H. Wang, C.U. Segre, J.R. Stetter, Humidity sensing properties of Nafion and sol-gel derived SiO<sub>2</sub>/Nafion composite thin films, *Sens. Actuators B* 40 (1997) 217–222.
- [27] J. Wang, Q. Lin, T. Zhang, R. Zhou, B. Xu, Humidity sensor based on composite material of nano-BaTiO<sub>3</sub> and polymer RMX, *Sens. Actuators B* 81 (2002) 248–253.
- [28] J. Wang, B.K. Xu, S.P. Ruan, S.P. Wang, Preparation and electrical properties of humidity sensing films of BaTiO<sub>3</sub>/polystyrene sulfonic sodium, *Mater. Chem. Phys.* 78 (2003) 746–750.

#### Biographies

**Pi-Guey Su** is currently a professor in Department of Chemistry at Chinese Culture University. He received his BS degree from Soochow University in Chemistry in 1993 and PhD degree in Chemistry from National Tsing Hua University in 1998. He worked as a researcher in Industrial Technology Research Institute, Taiwan, from 1998 to 2002. He joined as an assistant professor in the General Education Center, Chungchou Institute of Technology from 2003 to 2005. He worked as an assistant professor in Department of Chemistry at Chinese Culture University from 2005 to 2007. He worked as an associate professor in Department of Chemistry at Chinese Culture University from 2007 to 2010. His fields of interests are chemical sensors, gas and humidity sensing materials and humidity standard technology.

**Chuen-Chi Shiu** received a BS degree in Chemistry from Chinese Culture University in 2009. He entered the MS course of Chemistry at Chinese Culture University in 2009. His main areas of interest are gas sensing materials.